

Development of a Photo-Fenton Catalyst $\text{Fe}_3\text{O}_4/\text{TiO}_2$ Coated by Co polymer Synthesis by γ -rays

E. A. Hegazy, M. S. Abdel-Mottaleb*, H. A. Abd El-Rehim, and M. M. Ghobashy#

Radiation Research of Polymer Chemistry Dept., National Centre for Radiation Research and Technology (NCRRT), P.O. Box; 29 Nasr City, Cairo and *Chemistry dept., Faculty of Science, Ain Shams University, Cairo, Egypt. #E-mail; Mohamed_ghobashy@yahoo.com

PHOTO-FENTON CATALYSTS $\text{Fe}_3\text{O}_4/\text{TiO}_2$ coated with a co-polymer (PVA/PAAc) to improve their capabilities of pollutant degradation has been investigated. Core-shell nanocomposites catalyst $[(\text{Fe}_3\text{O}_4/\text{PAAc}/\text{PVA})/\text{TiO}_2]/\text{PAAc}$ with average diameters of 50-60 nm was carried out by gamma irradiation. Aqueous solution (1% w/v) of 25 % PVA/ 75% PAAc was polymerized at low irradiation doses 1.66 kGy, then treated with Fe^{2+} / Fe^{3+} salts. Ammonia solution was added to obtain a precipitation of 20 nm $\text{Fe}_3\text{O}_4/\text{PVA}/\text{PAAc}$. The Photo-Fenton catalysts comprising Fe_3O_4 nanoparticles as a core and (PVA/PAAc) as a shell and TiO_2 introduced, which later develop into a uniform polymer layer of PAAc. The polymer resembles a stabilizer for particles in nanosize without aggregation. The degradation of the Remazol Red dye (RR) dissolved in aqueous solutions was investigated using modified reactor contain ultra violet visible (UV-VIS) sources under the influence of 300 Gauss alternative magnetic field (M.F).

Keywords: Nanoparticles, Photo-Fenton reaction, polymer, γ -rays, magnetic oxide.

Removing of organic pollutant from water considered as one of the serious challenges facing the worldwide (Laisheng *et al.*, 2006). Recently, nanoparticles metal oxide semiconductors can be used to remove the organic pollutant by breaking their chemical bonds such as C—C , C—N , C—O and N—H when exposure to light with a certain wavelength resulting in CO_2 and H_2O . Photo catalytic reaction (Karamanisa *et al.*, 2011) with TiO_2 is well known methods for removing organic pollutant, it is non-toxic, chemically stable, cheap, and very efficient.

Fe_3O_4 have catalytic active sites for sensing hydrogen peroxide in the Fenton reaction (Chang and Ming, 2010) or Photo-Fenton reaction (Katsumata *et al.*, 2004), which is a new method of dye removing. The highly dispersion of TiO_2 in water restricted its re-usability. TiO_2 magnetic property was improved when it combined with other metal oxide like Fe_3O_4 , it has become more effective for degradation reaction (Xu *et al.*, 2012).

An energy gap of titanium dioxide, which has a crystalline ratio of (80 anatase: 20 rutile %) is 3.0-3.2 eV was sufficient for photonic activation (Bahnemann, 2004). This dictates that TiO_2 activated with light wavelength of down and/or up to 400 nm (Fujishima *et al.*, 2000). Meanwhile, Fe_3O_4 , show magnetic semiconductor with energy gap 2.8 eV. TiO_2 in the presence of Fe_3O_4 is red shifted and become active in the visible region and its super paramagnetic property was enhanced (Qinghang *et al.*, 2008). However, $\text{Fe}_3\text{O}_4/\text{TiO}_2$ unstable, where the photo generated electrons in the titanium dioxide phase being injected into the conduction band of the Fe_3O_4 core, leading the oxidization-reduction reaction between the TiO_2 and Fe_3O_4 results in a decrease in the dye degradation rate. Thus, directly depositing TiO_2 onto the surface of a magnetic Fe_3O_4 core proved to produce ineffective catalyst. The intermediate passive SiO_2 layer inhibited the direct contact between the titanium dioxide / ferric oxide-phases (Yu *et al.*, 2011) and hence prevented the photo dissolution of the Fe_3O_4 phase (Beydoun *et al.*, 2002). The new precipitated phase can originate as nanosize, which interact with and adhere to the surface of the seed particles. This is known as a heterocoagulation mechanism. This occurs when the system conditions allow for the interaction of the two different phases.

The challenge of the present work, find inert polymer surfaces that prevent hetero coagulation of titanium dioxide with the magnetite oxide where polymer can withstand reactive oxidative radicals attack during light, maintain adequate long-term catalytic stability, preclude the photocatalyst leaching during the light irradiation and allow the photocatalytic reaction to proceed with an acceptable kinetic (Zhiyong *et al.*, 2008). In this connection, $\text{TiO}_2/\text{Fe}_3\text{O}_4$ separated and coated with PVA and PAAc hydrophilic polymer prepared by γ -ray. The principal advantage of gamma irradiation method is that high monodisperse of $[(\text{Fe}_3\text{O}_4/\text{PAAc}/\text{PVA})/\text{TiO}_2]$ PAAc nanoparticles are carried out in polar solvent; water and $\text{TiO}_2/\text{Fe}_3\text{O}_4$ particles gain hydrophilic character when coating with *Egypt. J. Rad. Sci. Applic.*, Vol. 25, No. 1-2 (2012)

functioned hydrophilic copolymer. The morphological structure of the prepared catalyst $[(\text{Fe}_3\text{O}_4/\text{PAAc}/\text{PVA})/\text{TiO}_2]$ PAAc core-shell nanocomposites was characterized by X-ray diffraction (XRD). Catalytic activities of metal nanocomposites were studied against degradation dye of RR using modified reactor under the influence of the alternative (AC) magnetic field.

Materials and Methods

Azo-reactive dye; RR (1-Naphthalenesulfonic acid, 5-hydroxy-6-((2-methoxy-5-((2-(sulfooxy)ethyl)sulfonyl)phenyl)azo)-, disodium salt) from Aldrich (Germany). TiO_2 powder (Degussa, P-25), which is a standard material in the field of photocatalytic reactions, contains anatase and rutile phases in a ratio of about (80:20) %. $\text{FeSO}_4 \cdot 7\text{H}_2\text{O}$ and $\text{Fe}_2(\text{SO}_4)_3$ commercial trade with no further purification, The ferromagnetic Fe_3O_4 laboratory prepared, NH_4OH 30% from Aldrich (Germany), Polyvinyl alcohol (PVA) commercial with no further purification, Acrylic Acid (AAc) monomer, poly acrylic acid (PAAc) prepared by dissolving 30% AAc in acetone and irradiated for 10 kGy, after casting forming transparent PAAc film PAAc with molecular wt 10^5 . Schematic representation of the experimental setup for catalytic-reactor for pollutant removal by nanosized metal oxide polymer composite is shown in diagram.1. The laboratory-scale designed in column shaped 30cm height and 6cm diameter. Sealed and surrounded by copper coil to give alternative magnetic field by AC power supply and cooling by water to avoid any effect of temperature, sample exposure to magnetic field by passing through the column and return to beaker again in closed loop by peristaltic pump, the sample are exposure to 28W UV at 362nm and 8W Vis at range of 375-750nm, eliminated heat effect of the lamps by cooling fan, thus the temperature of the reaction medium was maintained constant at 30°C within $\pm 0.1^\circ\text{C}$. The intensity of irradiation entering the beaker is homogeneous by positing up of UV lamps and mirror downs the beaker

Polymer encapsulated Fe_3O_4 nanoparticles as core-shell structure has been obtained by directly dissolving of 1gm of $(\text{Fe}^{2+}:\text{Fe}^{3+})$ salts in a molar ratio (1.67:1) in 50 ml of 1% copolymer solution of (25% PVA-75% PAAc) irradiated 1.66 kGy (irradiation time 10 min). Good mixing by sonication. Dark precipitates of $(\text{Fe}_3\text{O}_4/\text{PVA-PAAc})$ were formed after 30% ammonia aqueous solution (NH_4OH) added into the reaction mixture.

Egypt. J. Rad. Sci. Applic., Vol. 25, No. 1-2 (2012)

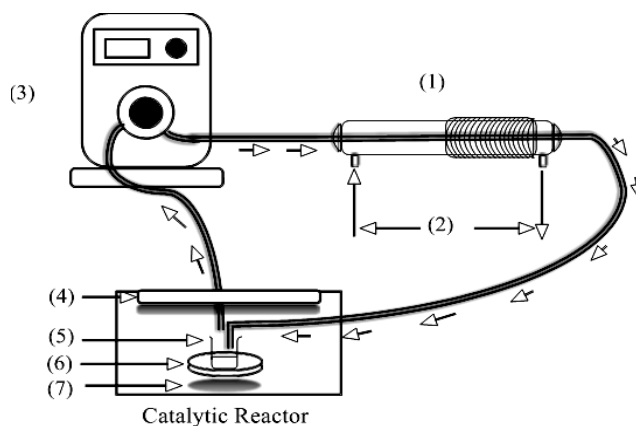


Diagram.1. Experimental setup for catalytic-reactor.

- (1) Magnetic field loop AC current coil. (2) Cooling water. (3) Peristaltic pump. (4) Ultra violet lamp. (5) Sample. (6) Fluorescent lamp. (7) Mirror.

The synthesis of dual metal oxide polymer composites catalyst $[(\text{Fe}_3\text{O}_4/\text{PAAc}/\text{PVA})/\text{TiO}_2]$ PAAc is the main target. Initially the black dark powder of $(\text{Fe}_3\text{O}_4 / \text{PVA-PAAc})$ at nanoscale was mixed with suspended TiO_2 (Degussa p-250) in the appropriate volume of water and leaving the stirrer run overnight. In a stepwise 2ml of AAc monomer has been added, forming layers of polymer held together by electrostatic interaction. After the mixing of polymers are completed and let stands overnight. The mixture re-irradiated with 50kGy, then produced a new hybrid capsules from hydrophilic polymer given core shell by $[(\text{Fe}_3\text{O}_4/\text{PAAc}/\text{PVA})/\text{TiO}_2]$ PAAc.

The catalytic activity of dual metal oxide was measured by the decay of absorbance peak of RR at $\lambda = 530 \text{ nm}$. 0.08g $[(\text{Fe}_3\text{O}_4/\text{PAAc}/\text{PVA})/\text{TiO}_2]$ PAAc was placed and mixed with $3 \times 10^{-5} \text{ M}$ of RR in a 50ml beaker of de-ionized water. The mixture kept in dark place for 30 min at the ambient temperatures for dye adsorption on the catalyst surface take place. The mixture exposed to 28W of UV lamp with range of $\lambda = 362\text{nm}$ and 8W of fluorescent lamp with range of $\lambda = 375\text{-}750 \text{ nm}$, Separated 3 ml of a sample from the mixture per time interval (10 min). Then, decolourization of RR was recorded during the decay of spectrum peak at 530nm on a UV-Vis spectrophotometer.

$$\text{Decolourization (\%)} = \frac{C_0 - C}{C_0} \times 100 \quad \dots\dots\dots (1)$$

Where, C_0 is the initial concentration of the dye and C is its concentration at each specified time.

Results and Discussion

Fig. 1a. and 1b. shows XRD patterns of $\text{Fe}_3\text{O}_4/\text{PVA}/\text{PAAc}$ and $[(\text{Fe}_3\text{O}_4/\text{PAAc}/\text{PVA})/\text{TiO}_2]$ PAAc nanoparticles respectively. Characteristic peaks for Fe_3O_4 at ($2\theta = 30.1^\circ, 35.5^\circ, 43.1^\circ, 53.4^\circ, 57.0^\circ$ and 62.6°) with hkl values (2 0 0), (3 1 1), (4 0 0), (4 2 2), (5 1 1), and (4 4 0) are observed for both samples. These peaks are consistent with the database in JCPDS file and reveal that Fe_3O_4 particles are in nanoscale according to Fe_3O_4 ; JCPDS 85-1436 (Le *et al.*, 2009). Fig. 1b. shows XRD patterns exhibited strong diffraction peaks at $27^\circ, 36^\circ$ and 55° indicating TiO_2 in the rutile phase and diffraction peaks at 25° and 48° indicating TiO_2 in the anatase phase. All peaks are in good agreement with the standard spectrum; JCPDS no.: 88-1175 and 84-1286 (Kheamrutai *et al.*, 2008).

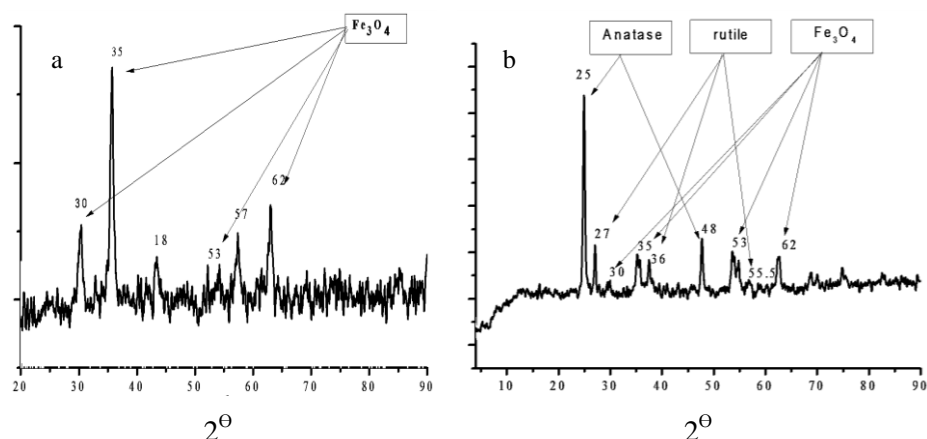


Fig. 1. XRD pattern: a) $\text{Fe}_3\text{O}_4/\text{PVA}/\text{PAAc}$ & b) $[(\text{Fe}_3\text{O}_4/\text{PAAc}/\text{PVA})/\text{TiO}_2]$ PAAc.

Energy-dispersive X-ray (EDX) were employed to identify $\text{Fe}_3\text{O}_4/\text{TiO}_2$ at $[(\text{Fe}_3\text{O}_4/\text{PAAc}/\text{PVA})/\text{TiO}_2]$ PAAc particle. Fig. 2a. shows the composition of synthesized $\text{Fe}_3\text{O}_4/\text{PVA}/\text{PAAc}$ nanoparticles and Fig. 2b. shown $\text{Fe}_3\text{O}_4 / \text{TiO}_2$ particle is capsulated with hydrophilic polymer. This assembly structure is similar to that reported below by Dynamic Light Scattering (DLS), Transmission Electron Microscope (TEM) and Atomic Force Microscope (AFM).

Direct way to determine particle size is the application of DLS supplied with analysis software. Fig. 3a. indicated that the nanospheres have excellent size homogeneity in aqueous medium and implied that the PVA/PAAc Fe_3O_4 with about 30 nm.

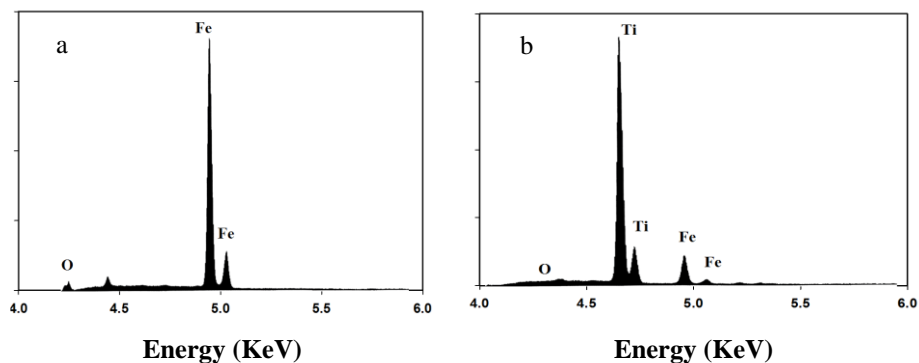


Fig. 2. EDX spectrum: a) Fe₃O₄/PVA/PAAc & b) [(Fe₃O₄/PAAc/ PVA)/TiO₂] PAAc.

Fig. 3b. shows the core shell of PVA/PAAc Fe₃O₄ was composed by TiO₂/PAAc with many homogeneous and produced closely packed with Fe₃O₄ nanoparticles [(Fe₃O₄/PAAc/ PVA)/TiO₂] PAAc to increase the size to 57nm.

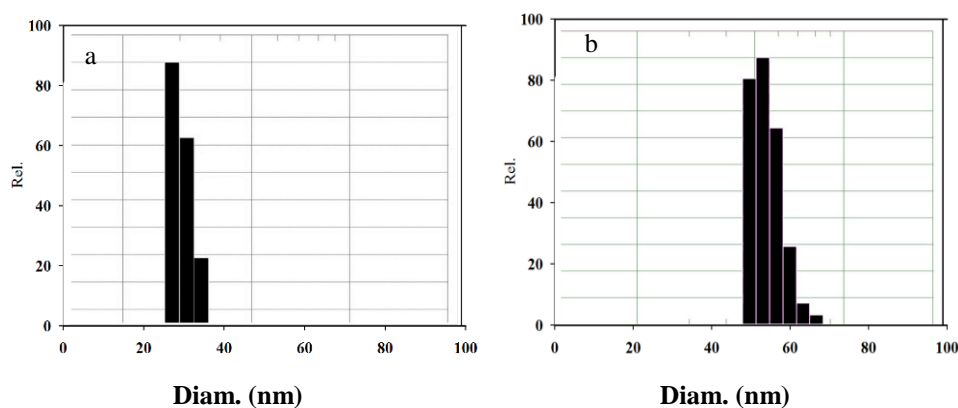


Fig. 3. Particle distribution: a) Fe₃O₄/PAAc/ PVA powders & b) [(Fe₃O₄/PAAc/ PVA)/TiO₂] PAAc.

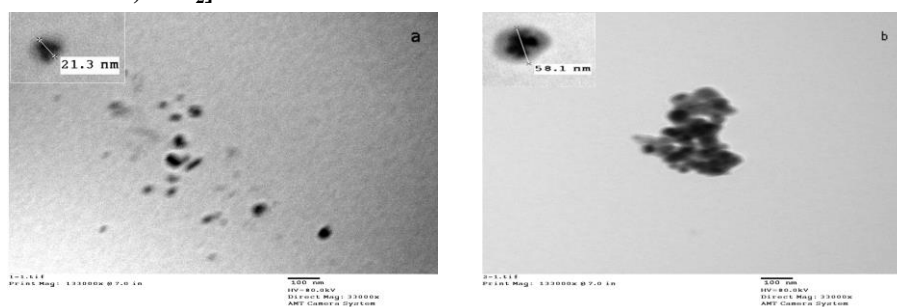


Fig. 4. TEM images: a) Fe₃O₄/PAAc/ PVA & b) [(Fe₃O₄/PAAc/ PVA)/TiO₂] PAAc.

Fig. 4a. shows TEM images of hydrophilic polymer PVA/PAAc capsulated Fe_3O_4 powders. The morphology of the coated particles is moderately spherical in shape and their mean diameter size is about 20-25 nm. Meanwhile, PVA/PAAc/ Fe_3O_4 and PAAc in Fig. 4b. TEM shows particles of $[(\text{Fe}_3\text{O}_4/\text{PAAc}/\text{PVA})/\text{TiO}_2]$ PAAc with mean diameter equal to 50-60 nm. The composite nanospheres had a perfect core shell structure.

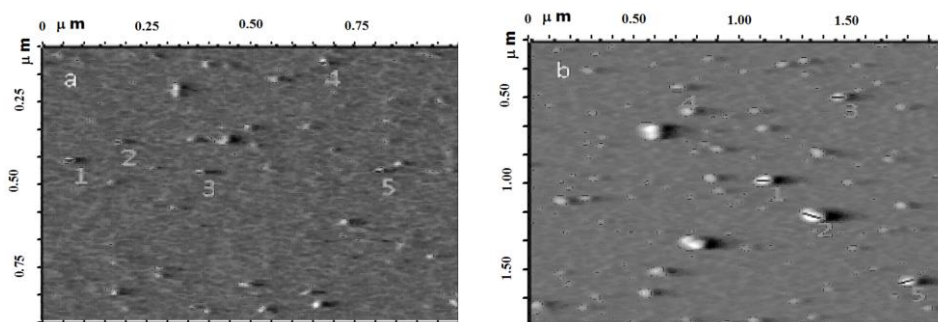


Fig. 5. Topographical scans for the surface: a) $\text{Fe}_3\text{O}_4/\text{PAAc}/\text{PVA}$ & b) $[(\text{Fe}_3\text{O}_4/\text{PAAc}/\text{PVA})/\text{TiO}_2]$ PAAc.

Fig. 5. shows supporting information to determine the morphology and particle size is the application of AFM, which give the surface morphology and size of PVA/PAAc/ Fe_3O_4 as shown in Fig. 5a. spherical with 20 nm size and Fig. 5b. TiO_2 inserts PVA/PAAc/ Fe_3O_4 followed by another layer of PAAc give rise to hollow spheres with sizes 60 still in the nanometer range is $[(\text{Fe}_3\text{O}_4/\text{PAAc}/\text{PVA})/\text{TiO}_2]$ PAAc, analyzed, and characterized through the determination of the appropriate scanning setting, the suitable data type imaging techniques and the most representative data analysis parameters using the AFM in contact mode. Photo-Fenton catalytic degradation activity of 0.08 g $[(\text{Fe}_3\text{O}_4/\text{PAAc}/\text{PVA})/\text{TiO}_2]$ PAAc towards 3×10^{-5} M RR could be measured using UV-VIS spectroscopy.

Fig. 6a. shows the UV spectrum of 3×10^{-5} M RR with strong absorption band at 530nm. The intensity of this band decreases as the reaction time increases. Under magnetic field influence, the red colour gradually decreases to reach 31.94 % after 50 min. The decrease of intense band can be attributed to the continuous degradation of dye in the presence of 0.08 g $[(\text{Fe}_3\text{O}_4/\text{PAAc}/\text{PVA})/\text{TiO}_2]$ PAAc under 300 Gauss magnetic field. Magnetic field enhances the diffusion of RR dye on coated polymer chains and accelerates the dye degradation rate on $[(\text{Fe}_3\text{O}_4/\text{PAAc}/\text{PVA})/\text{TiO}_2]$ PAAc surface.

Fig. 6b. showed the Photo-Fenton catalytic activities of [(Fe₃O₄/PAAc/PVA) /TiO₂] PAAc towards RR in the absence of magnetic field, the red colour gradually decreases to reach 21.57% after 50 min was convinced in Fig. 7. magnetic field enhanced degradation of RR specially in first 20 min the amount absorbed of dye increased the rate of decolourization reach to 26% while, in absent of magnetic field the rate of decolourization close to 3%.

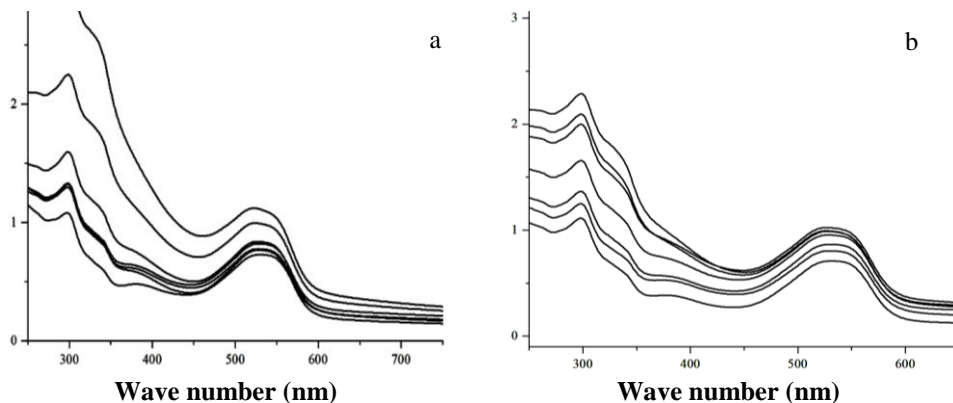


Fig. 6. UV-VIS Spectrophotometer of the degradation 3×10⁻⁵ M RR by catalyst composite of 0.08 g [(Fe₃O₄/PAAc/ PVA)/TiO₂] PAAc, temperature (30± 0.1 °C). a) Percent of AC magnetic field 300 Gauss (b) absent of AC magnetic field.

The problem for TiO₂ reusability limits its application in water treatment (Wu *et al.*, 2004). Meanwhile, the using of magnetic field considered as a good advantage to collect the [(Fe₃O₄/PAAc/PVA) /TiO₂]PAAc for further degradation. The kinetics of reaction were studied by the initial pH of the solution the pH of the reaction medium has a significant effect on the surface properties of the TiO₂/Fe₃O₄ catalyst. The rate of degradation of RR in aqueous suspensions of TiO₂:Fe₃O₄ has been studied in the pH ranged from 1 to 4. Therefore, the photocatalytic decolourization of RR is first-order reaction and its kinetic may also be expressed as follows;

$$\ln([C]) = \ln([C_0]) - k t \dots\dots\dots(2)$$

According to Eq. (1), Eq. (2) can also be expressed as follows:

$$\ln([A]) = \ln([A_0]) - k t \dots\dots\dots(3)$$

A plot of ln([A]) versus t is a straight line with slope-k. From experimental data the rate constant could be found from the slope of the appropriate plot. Fig. 8b. show the decolourization increased with pH up to pH 2 and then decreased, attaining maximum value of pH 2 due to pH altered the surface charge of TiO₂

catalyst and amount of dye adsorbed maximum at pH 2 where At pH > PZC (point of zero charge of metal oxide), the catalyst surface will be negatively charged and repulse the anionic dye compounds in water.

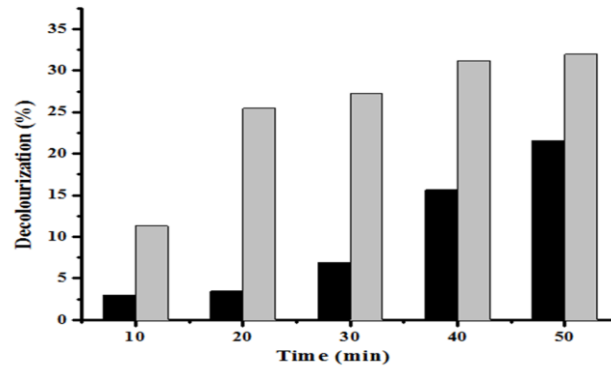


Fig. 7. The decolourization (%) of 3×10^{-5} M RR by 0.08g $[(\text{Fe}_3\text{O}_4/\text{PAAc}/\text{PVA})/\text{TiO}_2]$ PAAc, temperature (30 ± 0.1 °C) and pH 6.8.

- (■) Percent of 300 Gauss AC magnetic field
- (●) Absent of AC magnetic field.

At pH 3.5 the PZC for TiO_2 equal zero (Zeng *et al.*, 2008). The pH affects not only the surface properties of TiO_2 but also the dissociation of dye molecules and the formation of hydroxyl radicals.

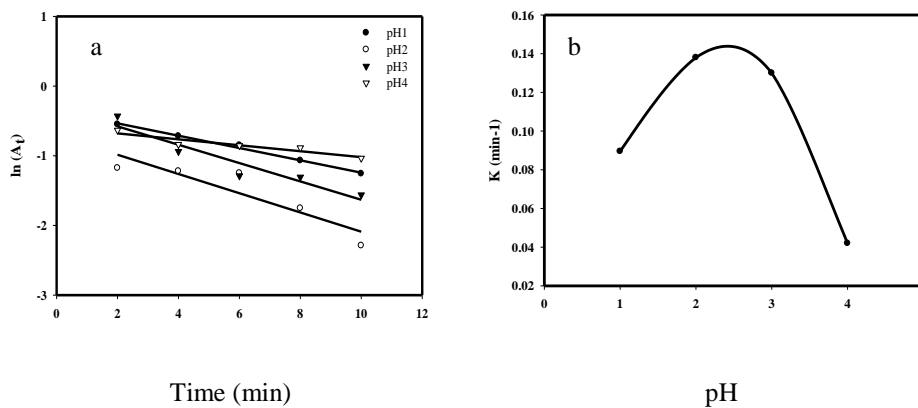


Fig. 8. catalytic degradation of 3×10^{-5} M RR at a) Influence of pH on 0.08g $[(\text{Fe}_3\text{O}_4/\text{PAAc}/\text{PVA})/\text{TiO}_2]$ PAAc and temperature (30 ± 0.1 °C). b) Variation of rate constant K (min^{-1}) with different pH at concentration 3×10^{-5} M of RR with 0.08 g $[(\text{Fe}_3\text{O}_4/\text{PAAc}/\text{PVA})/\text{TiO}_2]$ PAAc and temp (30 ± 0.1 °C).

Enforcement of the reaction rate under acid condition attributed to an increase in the concentration of hydroxonium ions, which initiated the degradation reaction (Akyol *et al.*, 2004, Lizama *et al.*, 2002 and Sakthivel *et al.*, 2003). Rate constant calculated from the plot of log absorbance vs. irradiation time, Fig. 8a. An indication that the reaction tends to first order reaction where $K = 0.146 \text{ min}^{-1}$.

Conclusions

Stabilizing of $\text{TiO}_2\text{:Fe}_3\text{O}_4$ nanoparticle in dispersion phase given the core shell ranged 21-57 nm achieved by polymer capsulation, to prevent the direct reaction of TiO_2 with Fe_3O_4 , which effectively in catalysis reaction, Fe_3O_4 nanoparticles induced magnetic effect on degradation enhancement, However, Fe_3O_4 nanoparticles tend to aggregate due to strong magnetic dipole-dipole attractions between particles so, modification of the surface of the Fe_3O_4 nanoparticles with polymer capsulated using gamma ray help for give good homogeneity in polymerization with constant rate. Concept of the photo-Fenton reaction depends on the production of hydroxyl radicals and the adsorption of reactant species on catalyst surface. Based on this concept the external AC magnetic field causing vibration motion of encapsulated catalyst and make ability to adsorption of dye on the surface of catalyst to increase the rate of decolourization from 3% to 26 % after 20 min and 21% to 31% after 50 min in absent and present of 300 Gauss AC magnetic field respectively, at pH2 the rate of decolourization reaches its maximum after 10 min given 88%, due to pH altered the surface charge of catalyst and adsorbed dye amount reach to maximum at pH 2 where at $\text{pH} > \text{PZC}(\text{metal oxide})$, the catalyst surface will be negatively charged and repulse the anionic dye compounds in water.

References

- Akyol, A., Yatmaz, H. C. and Bayramoglu, M. (2004) Photocatalytic decolorization of Remazol Red RR in aqueous ZnO suspensions. *Appl. Catal. B, Environ.*, **54**, 19.
- Bahnemann, D. (2004) Photocatalytic water treatment: solar energy applications. *Sol. Ene.*, **77**, 445.
- Beydoun, D., Rose, A., Gary, L. and Stephen, M. (2002) Occurrence and prevention of photodissolution at the phase junction of magnetite and titanium dioxide. *J. Mol. Catal. A-Chem.*, **180**, 193.
- Chang, M. W. and Ming C. M. (2010) Decolorization of peach red azo dye, HF6 by Fenton reaction: Initial rate analysis. *J. Taiwan Inst. Chem. Eng.*, **41**, 221.
- Fujishima, A., Tata, N., Rao, D. and Tryk, A. (2000) Titanium dioxide photocatalysis. *J. Photochem. Photobiol. C-Photo.*, **1**, 1.
- Egypt. J. Rad. Sci. Applic.*, Vol. 25, No. 1-2 (2012)

- Karamanisa, D., Ökteb, A. N., Vardoulakisa, E. and Vaimakisc, T. (2011)** Water vapor adsorption and photocatalytic pollutant degradation with TiO_2 -sepiolite nanocomposites *Appl. Clay Sci.*, **53**, 181.
- Katsumata, H., Shinsuke K., Satoshi, K., Tohru, S. and Kiyohisa, O. (2004).** Degradation of bisphenol in water by the photo-Fenton reaction. *J. Photochem. Photobiol. A: Chem.*, **162**, 297.
- Kheamrutai, T., Pichet, L. and Boonlaer, N. (2008)** Phase Characterization of TiO_2 Powder by XRD and TEM. *Nat. Sci.*, **42**, 357.
- Laisheng, L., Wanpeng, Z., Pengyi, Z., Qiuyun, Z. and Zulin, Z., (2006)** $\text{TiO}_2/\text{UV}/\text{O}_3$ -BAC processes for removing refractory and hazardous pollutants in raw water. *J. Haz. Mate.*, **128**, 145.
- Le, T. M., Tran, T. D., Tran, M. D., Nguyen, H., D. and Dang, M. C. (2009)** Preparation and characterization of magnetic nanoparticles coated with polyethylene glycol. *J. Phys. Conf. Series*, **187**, 589.
- Lizama, C., Freer, J., Baeza, J. and Mansilla, H. D. (2002)** Optimized photodegradation of reactive Blue 19 on TiO_2 and ZnO suspensions. *Catal. Today*, **76**, 235.
- Qinghang, H., Zhenxi, Z., Jianwen, X., Yuying, X. and Hua, X. (2008)** A novel biomaterial - $\text{Fe}_3\text{O}_4:\text{TiO}_2$ core-shell nano particle with magnetic performance and high visible light photocatalytic activity. *Opt. Mat*, **31**, 380.
- Yu, X., Shengwei, L. and Jiaguo, Y. (2011)** Superparamagnetic $\gamma\text{-Fe}_2\text{O}_3/\text{SiO}_2/\text{TiO}_2$ composite microspheres with superior photocatalytic properties. *App. Catal. B: Envir.*, **104**, 20.
- Sakthivel, S., Neppolian, B., Shankar, B. V., Arbindoo, B., Palanichamy, M. and Murugesan, V. (2003)** Solar photocatalytic degradation of azo dye: comparison of photocatalytic efficiency of ZnO and TiO_2 . *Sol. Energy Mater. Sol. Cells*, **77**, 65.
- Xu, P., Zeng, G., M., Huang, D., L., Feng, C., L., Hu, S., Zhao, M., H., Lai, C., Wei, Z., Huang, C. Xie, G., X. and Liu, Z., F. (2012)** Use of iron oxide nanomaterials in wastewater treatment. *Sci. Total Environ.*, **424**, 10.
- Wu, R., Qu, J. and He, H. (2004)** Removal of azo-dye Acid Red B (ARB) by adsorption and combustion using magnetic CuFe_2O_4 powder. *Appl. Catal. B.*, **48**, 49.
- Zeng, Y. P., Zimmermann, A., Aldinger, F. and Jiang, D. L. (2008)** Effect of organic additives on the zeta potential of PLZST and rheological properties of PLZST slurries. *J. Eur. Ceram. Soc.*, **28**, 2597.
- Zhiyong, Y., Laub, D., Bensimon, M. and Kiwi, J. (2008)** Flexible polymer TiO_2 modified film photocatalysts active in the photodegradation of azo-dyes in solution. *Inorg. Chim. Acta.*, **361**, 589.

(Received: 12/12/2012;

accepted: 24/02/2013)

Egypt. J. Rad. Sci. Applic., Vol. 25, No. 1-2 (2012)

تطوير الحفاز الفانتوني الضوئي من ثنائي أكسيد التيتانيوم وأكسيد الحديد الأسود المغلف بالبوليمر المحضر بأشعة جاما

السيد أحمد حجازي و محمد صبرى عبد المطلب* حسن أحمد عبد الرحيم
و محمد محمدى غباشى

قسم البحوث الإشعاعية لكيمياء البوليمرات ، المركز القومي لبحوث
و تكنولوجيا الإشعاع ، ص.ب. 29 مدينة نصر- القاهرة ، مصر ، و قسم الكيمياء
، كلية العلوم ، جامعة عين شمس ، القاهرة ، مصر .

تم تحضير مواد متقدمة من البوليمرات ذات المجموعات الوظيفية مترابطة مع بعض العناصر الانتقالية على هيئة دقائق كروية الشكل ذي الأبعاد النانو مترية محضره بأشعة جاما. تراوحت حجم الدقائق المتناهية الصغر من $[Fe_3O_4/PAAc/PVA)/TiO_2]PAAc$ حوالي ٥٠ نانوميتر. حيث أن وجود هذه الدقائق ولو بكميات قليلة تعمل على تحفيز عمليات تحلل الملوثات العضوية بطرق آمنة وبسيطة عن طريق إطلاق الكترولونات سالبه وفجوات موجبه و شوارد نشطه حره نتيجة امتصاص طاقه الفوتونات عند التعرض للأشعة فوق البنفسجية لتستخدم في تفاعل يسمى التحلل الفانتوني الضوئي. ويبرز دور البوليمرات في كونها تمتاز الملوثات المذابة لأنها ذي طبيعة محبه للماء تعمل على زيادة زمن التلامس بين الملوثات و الأكاسيد المختلطة الحفزية $(Fe_3O_4:TiO_2)$ وبالتالي تتم عملية التحلل في أقل زمن. وتم فحص فعالية هذه الدقائق على عملية التحلل للصبغة الحمراء بتركيز (10^{-3}) مولر عند التعرض للأشعة فوق بنفسجية تساوى ٣٦٢ نانومتر بقوة ٢٨ وات و أشعه مرئية اكبر من ٤٠٠ نانومتر بقوة ٨ وات مع استخدام الحث المغناطيسي المتردد ٣٠٠ جاوس زاد من ٣٪ إلى ٢٦٪ بعد ٢٠ دقيقة و من ٢١.٥٧٪ إلى ٣١.٩٤٪ في ٥٠ دقيقة مع إمكانية استعادة $(Fe_3O_4:TiO_2)$ باستخدام مغناطيس لإعادة الاستخدام الحافز عدة مرات وبنفس الكفاءة دون تغيير في الشكل الخارجي لثنائي أكسيد التيتانيوم و أكسيد الحديد الأسود.